

## Influence of $\text{Cu}(\text{NO}_3)_2$ Activator and Gas Composition on the Thermal Decomposition of Coal and Lignite

K. B. Larionov<sup>a, \*</sup>, I. V. Mishakov<sup>b, \*\*</sup>, K. V. Slyusarskiy<sup>a, \*\*\*</sup>,  
S. V. Lavrinenko<sup>a, \*\*\*\*</sup>, A. A. Gromov<sup>c, \*\*\*\*\*</sup>, and A. A. Vedyagin<sup>b, \*\*\*\*\*</sup>

<sup>a</sup>Tomsk Polytechnic University, Tomsk, Russia

<sup>b</sup>Boreskov Institute of Catalysis, Novosibirsk, Russia

<sup>c</sup>Moscow Institute of Steel and Alloys, Moscow, Russia

\*e-mail: laryk070@gmail.com

\*\*e-mail: mishakov@catalysis.ru

\*\*\*e-mail: slyuskonst@gmail.com

\*\*\*\*e-mail: serg86@tpu.ru

\*\*\*\*\*e-mail: alexandergromov1@gmail.com

\*\*\*\*\*e-mail: vedyagin@catalysis.ru

Received September 25, 2019; revised September 25, 2019; accepted October 21, 2019

**Abstract**—The thermal transformation of coal and lignite in the presence of  $\text{Cu}(\text{NO}_3)_2$  activator (5 wt %) is investigated as a function of the atmospheric composition. The copper nitrate is supported on to the samples by the incipient wetness with  $\text{Cu}(\text{NO}_3)_2$  solution in water and alcohol. The effect of the activator is studied as a function of the gas (air/argon) composition, by thermogravimetric analysis with heating at  $10^\circ\text{C}/\text{min}$  in the range  $25\text{--}800^\circ\text{C}$ , at atmospheric pressure. With change in gas composition, the activity of  $\text{Cu}(\text{NO}_3)_2$  changes. Specifically, the thermal transformation is shifted to lower temperature:  $\Delta t = 33^\circ\text{C}$  for lignite and  $70^\circ\text{C}$  for coal. With increase in oxidant (air) content in the gas, the activity of the added  $\text{Cu}(\text{NO}_3)_2$  increases: that is,  $\Delta t$  increases. By mass spectrometry, the gaseous oxidation products of the coal are analyzed. The upper temperature limits on the peaks of nitrogen-oxide ( $\text{NO}_x$ ) liberation are determined as a function of the gas composition.

**Keywords:** coal, lignite, oxidation temperature, activated oxidation, copper nitrate, thermogravimetric analysis, mass-spectrometric analysis, gas composition

**DOI:** 10.3103/S1068364X20030035

The catalytic combustion of coal is a promising means of converting solid fuel to thermal energy. The degree of coal conversion is high thanks to activation of combustion at relatively low temperature. That also minimizes the pollutant yield in the exhaust gases [1–4]. Most research concentrates on the use of metal oxides to accelerate the oxidation of the organic fuel [5–9].

The precursors of metal oxides (metal salts) have greater action on the thermal conversion of coal, as established in [10–12]. Specifically, the conversion temperature is lowered, and the liberation of volatiles is accelerated. We assume that the intensification of coal oxidation in the presence of precursors is associated with decomposition of the salt in the first stage of sample heating (to  $200^\circ\text{C}$ ) and the formation of metal oxide ( $\text{CuO}_x$ ), which catalyzes the complete oxidation of organic substrates [13].

The catalytic activity of metal oxides may be regulated by adjusting the gas composition (the  $\text{O}_2/\text{N}_2$  ratio), according to [14]. The research showed that

increase in the  $\text{O}_2/\text{N}_2$  ratio in the gas flux (increase in its oxidative character) intensifies the activity of the catalytic oxide additives, which lower the temperature at which intense oxidation begins and hasten the thermal decomposition of coal. For coal samples of little metamorphic development (lignite), the temperature at which volatiles are released under the action of  $\text{CuSO}_4$  additive changes more significantly in an inert atmosphere, as shown in [11].

In the present work, we study experimentally the influence of added  $\text{Cu}(\text{NO}_3)_2$  activator on the thermal conversion of lignite and coal, with variation in gas composition.

### EXPERIMENTAL MATERIALS AND METHOD

The initial samples are as follows: 2B lignite (Borodinsk field) and T coal (Alardinsk field). Initial coal samples of size 5–10 mm are crushed in drum mills for 8 h with a 1 : 1 mass ratio of the crushing balls and coal. The samples are then sorted on screens with  $80\text{-}\mu\text{m}$

**Table 1.** Characteristics of samples

Sample	Technical analysis, %				Elemental analysis, wt %					Moisture content, mL/g	Content, % in size class, $\mu\text{m}$			
	$W^r$	$A^r$	$V^r$	$C^r$	$C^{\text{daf}}$	$H^{\text{daf}}$	$N^{\text{daf}}$	$S^{\text{daf}}$	$O^{\text{daf}}$		$X_{10}$	$X_{50}$	$X_{90}$	$X_{\text{me}}$
2B lignite	1.0	4.5	39.8	54.7	59.4	5.3	1.7	0.9	32.7	3.4	2.8	13.9	34.8	18.3
T coal	0.3	16.5	13.1	70.1	80.0	2.8	2.5	0.4	14.3	2.6	4.6	20.4	57.6	26.5

As a preliminary, the coal powder is dried at  $105^\circ\text{C}$  to constant mass.

cells. Table 1 presents the size distribution of the coal particles, according to an Analysette 22 laser-diffraction instrument (Fritsch, Germany).

Although the samples are prepared by the same method, the mean particle diameter varies from  $18.3 \mu\text{m}$  (2B lignite) to  $26.3 \mu\text{m}$  (T coal). This may be explained by the different structure and morphology of the coal and lignite [15]. Table 1 also presents the technical analysis and elemental analysis of the samples; standard methods are employed [16]. The content of the basic elements (C, H, N, S, and O) in the samples is determined by means of a Euro EA 3000 analyzer (EuroVector, Italy).

The initial lignite and coal samples are very different in their physicochemical properties (Table 1). For example, the lignite has high content of volatiles ( $\sim 40\%$ ) and a relatively low ash content (no more than 5 wt %). That is associated with the limited metamorphic development. The T coal, by contrast, has low content of volatiles ( $\sim 13\%$ ) and high ash content (16.0 wt %) and carbon content ( $\sim 80\%$ ).

The  $\text{Cu}(\text{NO}_3)_2 \cdot 3\text{H}_2\text{O}$  activator is introduced in the samples by incipient wetness procedure [17]. To prevent hydrophobic behavior of the coal powder, a water/alcohol ( $\text{C}_2\text{H}_5\text{OH}$ ) mixture (50 : 50, by volume) is employed. The moisture content of the dried coal samples (mL/g) is determined immediately before deposition (Table 1). Then the solution is applied to the coal powder by mechanical dosing. The steeped samples are held in the drying chamber at  $105^\circ\text{C}$  for 20 h. The  $\text{Cu}(\text{NO}_3)_2 \cdot 3\text{H}_2\text{O}$  content in the modified sample is 5 wt % (recalculated for dry salt). For comparison, we prepare control samples without  $\text{Cu}(\text{NO}_3)_2$  activator, which undergo exactly the same treatment. The modified coal and lignite samples are denoted by C/Cu and L/Cu, respectively.

A Jupiter STA 449C synchronous thermal analyzer (Netzsch, Germany) is used to study the thermal transformation of the modified samples in identical conditions at atmospheric pressure. The  $\sim 15$ -mg sample is heated in a corundum crucible with a perforated lid in the range  $25$ – $800^\circ\text{C}$  at  $10^\circ\text{C}/\text{min}$ . The gas (air + argon) is supplied at a rate of 200 mL/min. The air/argon ratio varies as follows: 10/90, 30/70, 50/50, 70/30, and 90/10.

The  $\text{NO}_x$  liberation is recorded by means of a QMS 403D Aeolus (Netzsch, Germany) quadrupole mass-spectrometer.

The following characteristics of thermal transformation are determined: the initial  $t_i$  and final  $t_f$  temperatures of the process; the maximum reaction rate  $w_{\text{max}}$  at the corresponding temperature  $t_{\text{max}}$ ; the time  $T_e$  for which the sample is heated before decomposition begins; the total time  $T_f$  of thermal decomposition; and the time  $T_{\text{max}}$  to reach the maximum reaction rate. These parameters are calculated from the measurement results by a graphical method (described in detail in [10]).

For the T coal samples with bimodal differential thermal gravimetric (DTG) curves, this range is divided into two: 1) emission of volatiles; 2) oxidation of the coke residue.

## RESULTS AND DISCUSSION

In Figs. 1 and 2, we show TG and DTG curves for the samples in atmospheres of different compositions. We see that, in all cases, the  $\text{Cu}(\text{NO}_3)_2$  activator markedly changes the process: the temperature  $t_i$  at which thermal transformation begins is lowered.

The thermal decomposition of coal in analogous consists of 3–4 main stages (depending on the coal rank), according to [10–12]. These stages are associated with the evaporation of physically adsorbed water, the vaporization and oxidation of volatiles, and the oxidation of the coke residue.

With increase in content of the inert gas (argon), thermal decomposition of the unmodified samples is shifted to higher temperatures (Figs. 1 and 2). In the presence of  $\text{Cu}(\text{NO}_3)_2$  activator, the displacement of the TG and DTG curves is less pronounced. That may be associated with activation of the thermal transformation as a result of decomposition of the added  $\text{Cu}(\text{NO}_3)_2$  in the low-temperature region ( $\sim 200^\circ\text{C}$ ).

In Figs. 3 and 4, we show the change in the thermal decomposition of the samples with variation in gas composition.

It is evident that, in all cases, the initial  $t_i$  (Fig. 3a) and final  $t_f$  (Fig. 3b) temperatures of thermal decomposition are decreased as the oxidant content in the gas increases. Note that the final decomposition temperature cannot be recorded in the gas with the maximum

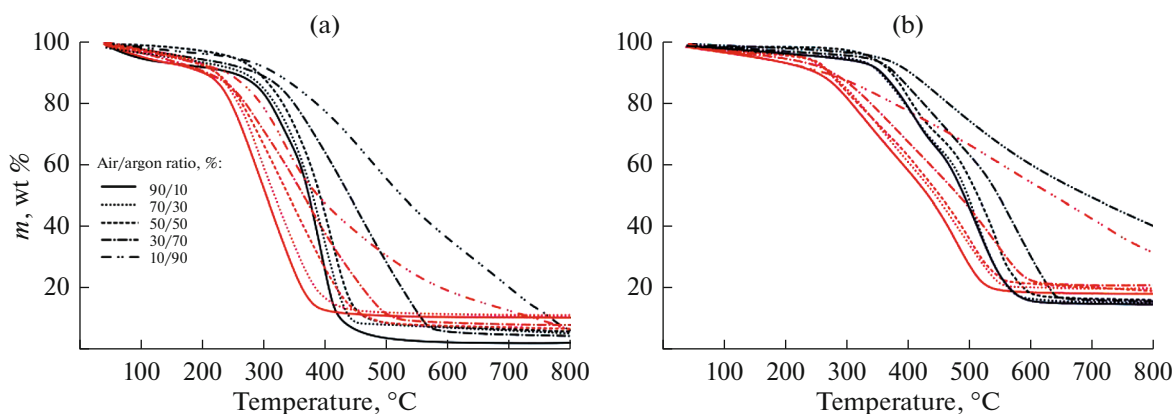


**Fig. 1.** Thermogravimetric (TG) data for the thermal decomposition of 2B lignite (a) and T coal (b) samples in the presence (red curves) and absence (black curves) of  $\text{Cu}(\text{NO}_3)_2$  activator in mixtures of air and argon (supplied at 200 mL/min) with heating at  $10^\circ\text{C}/\text{min}$ .

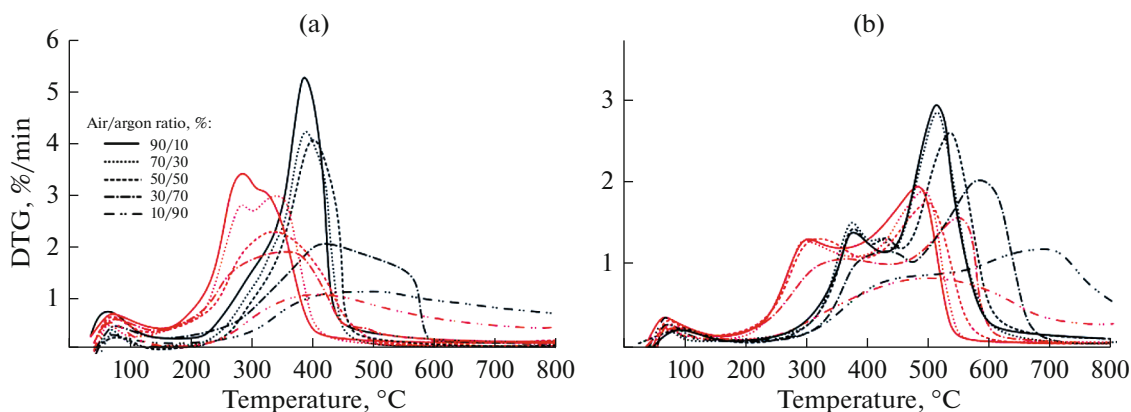


**Fig. 2.** DTG data for the thermal decomposition of 2B lignite (a) and T coal (b) samples in the presence (red curves) and absence (black curves) of  $\text{Cu}(\text{NO}_3)_2$  activator in mixtures of air and argon (supplied at 200 mL/min) with heating at  $10^\circ\text{C}/\text{min}$ .

argon content (90%), since the total mass loss in the given range  $25\text{--}800^\circ\text{C}$  (Fig. 3b) is no more than 70% for 2B lignite and 50% for T coal.

The greatest displacement of  $t_i$  ( $\Delta t = 70^\circ\text{C}$ ) is observed for the modified T coal sample with a 90 : 10 air/argon ratio. In that case, it is also found that, with increase in oxygen content in the gas, the activity of the added  $\text{Cu}(\text{NO}_3)_2$  declines. For the lignite sample, different behavior is observed: stronger influence of  $\text{Cu}(\text{NO}_3)_2$  on the yield of volatiles and their subsequent oxidation. This is most likely associated with the nonuniform lignite structure and a greater quantity of lateral bonds and crosslinks, in the form of oxygen-bearing molecular groups [18]. Such groups actively react with nitrogen oxides to form copper nitrite [19].

Note the symbatic variation of the heating time  $T_e$  before oxidation of the volatiles and the parameter  $t_i$  (Fig. 3a), since the temperature at the onset of sample heating is  $25^\circ\text{C}$ . The total oxidation time of the active sample mass  $T_f$  (oxidation of the volatiles and the coke

residue) behaves differently (Fig. 3b). For example, with increase in argon content,  $t_f$  and  $T_f$  increase. That may indicate decrease in the sample's mean decomposition rate. With maximum air content in the gas mixture, the decrease in  $t_f$  is greatest (Fig. 3b). Thus,  $\Delta T_f$  is 1 min for the modified T coal sample and 5 min for the modified lignite sample. The increase in transformation rate may be associated with the stronger reaction between the oxidative medium and the liberated nitrogen oxides and the nonstoichiometric carbon oxide formed [13]. That is typical of high activity in the oxidation of a combustible substrate.

With increase in oxidant content in the gas,  $T_{\text{max}}$  is displaced downward (Fig. 4a). The displacement of  $t_{\text{max}}$  between the maximum and minimum oxidant content in the gas is  $51^\circ\text{C}$  for the unmodified T coal sample and  $75^\circ\text{C}$  for the unmodified 2B lignite sample. Note also that, for the samples with bimodal DTG curves, the parameters in Fig. 4 correspond to the first maximum, characterizing the oxidation of volatiles.

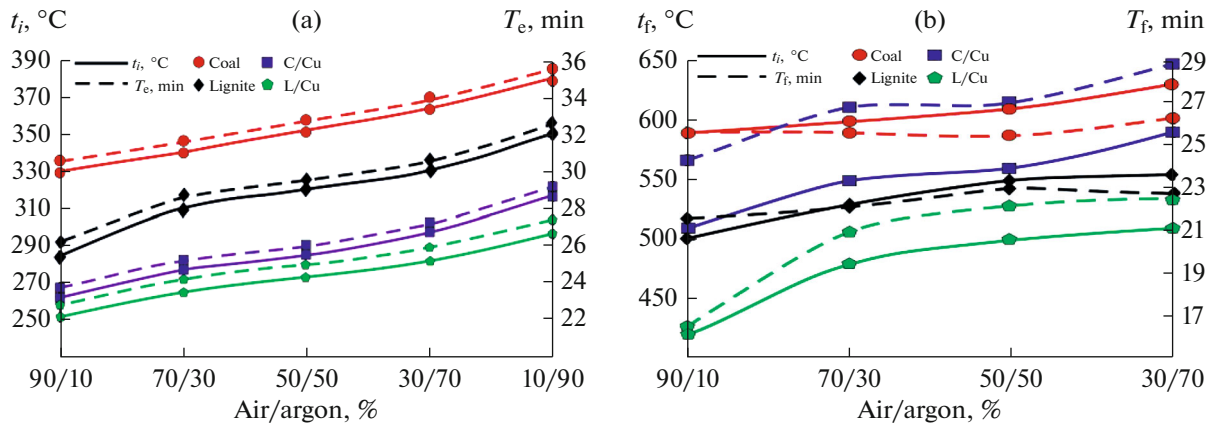


**Fig. 3.** Influence of the gas composition on the initial decomposition temperature  $t_i$  and time  $T_e$  (a) and final decomposition temperature  $t_f$  and time  $T_f$  (b) of the modified and unmodified T coal and 2B lignite samples, according to data from the synchronous thermal analyzer.

For the modified T coal and 2B lignite samples, the change in  $t_{\max}$  is practically the same:  $\sim 110^\circ\text{C}$ . With increase in argon content in the gas, the difference  $\Delta t_{\max}$  between the modified and unmodified samples decreases (Fig. 4a). Thus, with maximum oxidant content in the gas,  $\Delta t_{\max}$  is  $115^\circ\text{C}$  for the T coal and

$60^\circ\text{C}$  for 2B lignite. With the minimum oxidant content in the gas,  $\Delta t_{\max}$  is  $71^\circ\text{C}$  for the T coal and  $30^\circ\text{C}$  for 2B lignite.

With increase in argon content, the time  $T_{\max}$  to reach the maximum oxidation rate for modified samples begins to behave analogously to  $t_{\max}$  (Fig. 4a). This is associated with decrease in the influence of the added  $\text{Cu}(\text{NO}_3)_2$  on the rate of oxidation of the volatiles. Note also that the change in  $t_{\max}$  is greatest for the T coal samples in gas with maximum oxidant content: for modified T coal,  $\Delta T_{\max} = 4.5$  min. For modified lignite,  $\Delta T_{\max} = 3$  min.

With minimum oxidant content in the gas,  $\Delta T_{\max}$  becomes negative for T coal. For modified lignite, by contrast, the maximum effect is observed with a 1 : 1 air/argon ratio (Fig. 4a).

With increase in argon content in the gas (Fig. 4b), the maximum oxidation rate  $w_{\max}$  declines. This is most evident for the T coal samples, for which the variation in  $w_{\max}$  is nonlinear. When the air/argon ratio is 30/70, we note sharp decrease in  $w_{\max}$  in comparison with the 50/50 mixture:  $\Delta w_{\max} = 1.7\%/min$ . That is comparable with the change in  $t_{\max}$  and  $T_{\max}$  (Fig. 4a).

On modifying the samples with  $\text{Cu}(\text{NO}_3)_2$ , the maximum oxidation rate declines as a result of the intensification of oxidation and its displacement to lower temperatures (Fig. 4b). The difference in  $w_{\max}$  on modifying the T coal with  $\text{Cu}(\text{NO}_3)_2$  is approximately the same for any gas composition:  $\Delta w_{\max} = 0.2\%/min$ .

In Fig. 5, we show mass-spectrometric data for the nitrogen oxides formed in the thermal decomposition of the samples. With decrease in oxidant content in the gas, the temperature of maximum  $\text{NO}_x$  liberation ( $m/z = 30$ ) in  $\text{Cu}(\text{NO}_3)_2$  decomposition rises. This is most evident for the modified lignite, for which the tem-

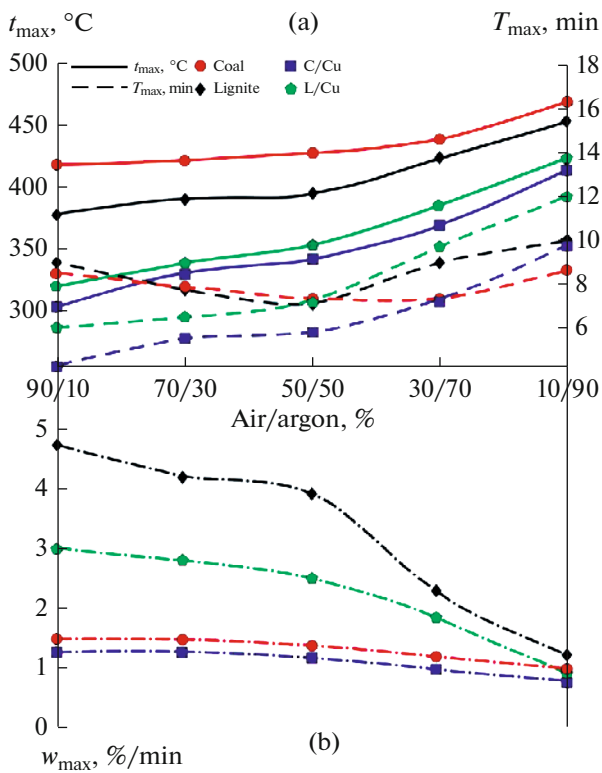


**Fig. 4.** Influence of the gas composition on the sample's rate of maximum mass loss  $w_{\max}$  (b) and the corresponding time  $T_{\max}$  and temperature  $t_{\max}$  (a), according to data from the synchronous thermal analyzer.

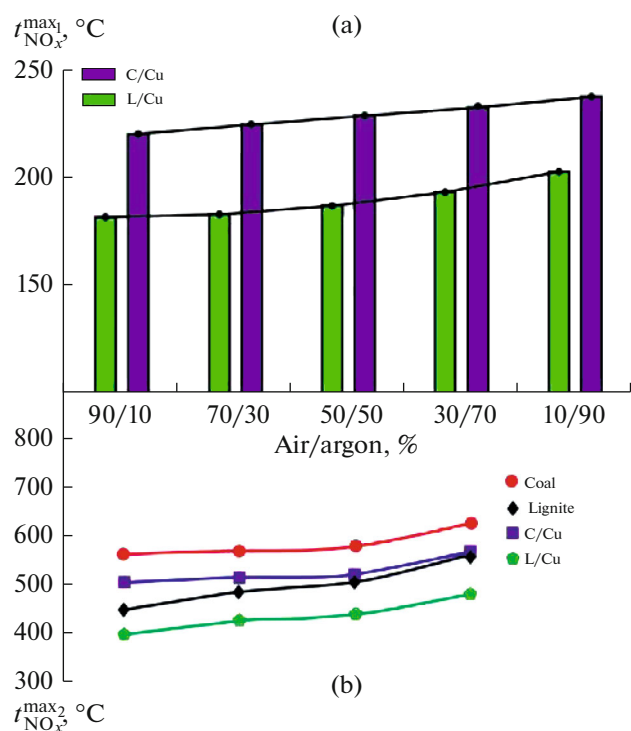


**Fig. 5.** Influence of the air/argon ratio in the atmosphere (supplied at 200 mL/min) on the temperature corresponding to the maximum rate of NO<sub>x</sub> liberation from copper nitrate in the lower range (a) and in the higher range (b), according to mass-spectrometric data: heating rate 10°C/min; temperature 25–800°C.

perature shift is 20°C. For the T coal sample, the corresponding shift is 17°C.

The mean difference  $\Delta t_{NO_x}^{max_1}$  between the modified samples is 38.8°C. The difference in the temperatures corresponding to the maximum rate of NO<sub>x</sub> liberation from copper nitrate may be attributed to the different morphology of the samples. Lignite has a nonuniform structure with numerous open pores and channels and has lower diffusional drag when gas flows past the sample, according to [20]. That permits greater interaction of the oxidant with nitrate integrated into the coal sample by capillary steeping, which intensifies the decomposition.

Comparison of the results from the synchronous thermal analyzer (Fig. 4a) and the mass-spectrometric data (Fig. 5) indicates that  $\Delta t_i$  is directly correlated with the temperature  $\Delta t_{NO_x}^{max_1}$  corresponding to maximum NO<sub>x</sub> liberation from copper nitrate.

For the subsequent NO<sub>x</sub> liberation in the high-temperature region (400–600°C), the temperature  $\Delta t_{NO_x}^{max_2}$  increases with decrease in oxidant content in the gas. Note that, for the lignite samples, the activity of the Cu(NO<sub>3</sub>)<sub>2</sub> is increased in the case, as is evident

from the increase in the difference  $\Delta t_{NO_x}^{max_2}$  between the modified and unmodified samples (53–85°C). The temperature shift  $\Delta t_{NO_x}^{max_2}$  for the T coal samples is practically independent of the gas composition, remaining at 56°C.

## CONCLUSIONS

We have investigated the thermal transformation of coal and lignite in the presence of Cu(NO<sub>3</sub>)<sub>2</sub>, as a function of the atmospheric composition (the air/argon ratio). We find that increase in the oxidant content in the gas sharply changes the thermal transformation. We may note the following aspects of this change:

- (1) shift in the process to lower temperature ( $\Delta t = 70^\circ\text{C}$ );
- (2) increase in rate of the process ( $\Delta w = 1.7\%/min$ );
- (3) decrease in heating time to volatile liberation ( $\Delta T_e = 7 min$ );
- (4) shift in oxidation to lower temperatures;
- (5) greater catalytic effect of Cu(NO<sub>3</sub>)<sub>2</sub>: in particular decrease in the initial temperature of active oxidation.

It follows from mass-spectrometric analysis that, with decrease in oxidant content in the gas, the temperature corresponding to maximum rate of NO<sub>x</sub> liberation from copper nitrate Cu(NO<sub>3</sub>)<sub>2</sub> increases. The peak of the second stage NO<sub>x</sub> liberation is also shifted to higher temperatures.

## ACKNOWLEDGMENTS

Financial support was provided by the Russian President (project NSh-2513.2020.8) and the Russian Ministry of Education and Science (project 0303-2016-0014).

## REFERENCES

1. Zyryanova, M.M., Badmaev, S.D., Belyaev, V.D., et al., Catalytic conversion of hydrocarbon raw material into fuel for power plants, *Katal. Prom-sti*, 2013, no. 3, pp. 22–27.
2. Sidorov, A.D., Fedorov, I.A., Dubinin, Yu.V., et al., Catalytic thermal systems for industrial heating, *Katal. Prom-sti*, 2012, no. 3, pp. 50–57.
3. Parmon, V.N., Simonov, A.D., Sadykov, V.A., and Tikhov, S.F., Catalytic combustion: Achievements and problems, *Combust., Explos., Shock Waves*, 2015, vol. 51, no. 2, pp. 143–150.
4. Tikhov, S.F., Simonov, A.D., Yazykov, N.A., et al., Catalytic combustion of brown coal particulates over ceramometal honeycomb catalyst, *Catal. Sustainable Energy*, 2012, vol. 1, pp. 82–89.

5. Gong, X., Guo, Z., and Wang, Z., Reactivity of pulverized coals during combustion catalyzed by  $\text{CeO}_2$  and  $\text{Fe}_2\text{O}_3$ , *Combust. Flame*, 2010, vol. 157, pp. 351–356.
6. Gong, X., Guo, Z., and Wang, Z., Variation on anthracite combustion efficiency with  $\text{CeO}_2$  and  $\text{Fe}_2\text{O}_3$  addition by differential thermal analysis (DTA), *Energy*, 2010, vol. 35, pp. 506–511.
7. Gong, X., Guo, X., and Wang, Z., Variation of char structure during anthracite pyrolysis catalyzed by  $\text{Fe}_2\text{O}_3$  and its influence on char combustion reactivity, *Energy Fuels*, 2009, vol. 23, pp. 4547–4552.
8. Wei, L., Zhang, N., and Yang, T., Effects of alkaline earth metal on combustion of pulverized coal, *Adv. Mater. Res.*, 2012, vols. 516–517, pp. 271–275.
9. Huang, C.J., Wang, S.J., Wu, F., et al., The effect of waste slag of the steel industry on pulverized coal combustion, *Energy Sources, Part A*, 2013, vol. 35, pp. 1891–1897.
10. Larionov, K.B. and Gromov, A.A., Non-isothermal oxidation of coal with  $\text{Ce}(\text{NO}_3)_3$  and  $\text{Cu}(\text{NO}_3)_2$  additives, *Int. J. Coal Sci. Technol.*, 2019, vol. 6, no. 1, pp. 37–50.
11. Larionov, K.B., Mishakov, I.V., Vedyagin, A.A., and Gubin, V.E., Effect of an initiating additive of  $\text{CuSO}_4$  on changes in the characteristics of brown coal oxidation and pyrolysis, *Solid Fuel Chem.*, 2019, vol. 53, no. 2, pp. 120–127.
12. Larionov, K.B., Mishakov, I.V., Styusarskii, K.V., et al., Intensification of the oxidation of lignite and coal by an activating additive of  $\text{Fe}(\text{NO}_3)_2$ , *Solid Fuel Chem.*, 2019, vol. 53, no. 5, pp. 262–269.
13. Wang, Y., Wang, J., Chen, H., et al., Preparation and  $\text{NO}_x$ -assisted soot oxidation activity of a  $\text{CuO}-\text{CeO}_2$  mixed oxide catalyst, *Chem. Eng. Sci.*, 2015, vol. 135, pp. 294–300.
14. Liu, G., Liao, Y., Guo, S., et al., Thermal behavior and kinetics of municipal solid waste during pyrolysis and combustion process, *Appl. Therm. Eng.*, 2016, vol. 98, pp. 400–408.
15. Epshtein, S.A., Crack formation in different type coals, *Gorn. Inf.-Anal. Byull.*, 2009, no. 9, pp. 71–76.
16. Tabakaev, R., Kanipa, I., Astafev, A., et al., Thermal enrichment of different types of biomass by low-temperature pyrolysis, *Fuel*, 2019, vol. 245, pp. 29–38.
17. Tokareva, I.V., Mishakov, I.V., Korneev, D.V., et al., Nanostructuring of the carbon macrofiber surface, *Nanotechnol. Russ.*, 2015, vol. 10, pp. 158–164.
18. Wang, D.M., Xin, H.H., Qi, X.Y., et al., Reaction pathway of coal oxidation at low temperatures: A model of cyclic chain reactions and kinetic characteristics, *Combust. Flame*, 2016, vol. 163, pp. 447–460.
19. Morozov, I.V., Znamenkov, K.O., Korenev, Yu.M., and Shlyakhtin, O.A., Thermal decomposition of  $\text{Cu}(\text{NO}_3)_2 \cdot 3\text{H}_2\text{O}$  at reduced pressures, *Thermochim. Acta*, 2003, vol. 403, pp. 173–179.
20. Strakhov, V.M., Kashlev, I.M., Soloviev, M.A., and Surovtseva, I.V., Changes in lignite on industrial storage, *Coke Chem.*, 2017, vol. 60, no. 2, pp. 47–54.

Translated by B. Gilbert